Spectrochimica Acta Part A: Molecular and Biomolecular Spectroscopy 251 (2021) 119487

Contents lists available at ScienceDirect

Spectrochimica Acta Part A: Molecular and Biomolecular Spectroscopy

journal homepage: www.elsevier.com/locate/saa

Synthesis, characterization and the nonlinear optical properties of newly synthesized 4-((1,3-dioxo-1-phenylbutan-2-yl)diazenyl) benzenesulfonamide

H.A. Sultan [a], Adil Muala Dhumad [b], Qusay M.A. Hassan [a,*], Tarek Fahad [b], C.A. Emshary [a], Nabeel A. Raheem [b]

[a] Department of Physics, College of Education for Pure Sciences, University of Basrah, Basrah 61001, Iraq
[b] Department of Chemistry, College of Education for Pure Sciences, University of Basrah, 61001, Iraq

HIGHLIGHTS

- The azo compound was prepared by coupling reaction of dizonium salt of sulfanilamide with benzoylacetone.
- We studied the nonlinear optical properties of azo compound.
- The nonlinear refractive index of this sample is determined using diffraction ring patterns and Z-scan techniques.
- The sample exhibits self-diffraction ring patterns due self-phase modulation.

GRAPHICAL ABSTRACT

Optimized structure of azo compound NA4.

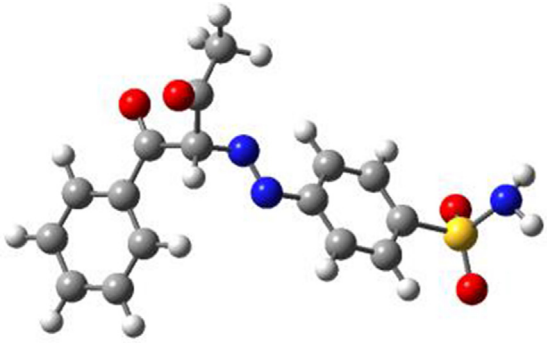

ARTICLE INFO

Article history:
Received 6 November 2020
Received in revised form 6 January 2021
Accepted 11 January 2021
Available online 15 January 2021

Keywords:
Azo compound
Z-scan
Nonlinear refractive index
Optical limiting
Optical materials

ABSTRACT

The dye of azo compound is prepared by coupling reaction of dizonium salt of sulfanilamide with benzoylacetone. The product is characterized by FTIR spectroscopy, Mass spectroscopy and ^{1}H NMR spectroscopy. The geometries of the synthesized dye is optimized using B3LYP method and 6-31G (d,p) basis sets. Nonlinear optical properties are investigated theoretically by calculation of some quantum chemical descriptors using the DFT/B3LYP method with a 6-31G(d,p) basis set in comparison with urea as a standard. The UV–visible spectrum of synthesized azo dye are calculated using TD-DFT with B3LYP/6-31G(d,p) level. The nonlinear refractive index of the prepared dye is calculated via the diffraction ring patterns and Z-scan techniques using 473 nm visible, continuous wave laser light. The diffraction ring patterns are numerically simulated using the Fresnel-Kirchhoff theory with reasonable agreements. The property of optical limiting of the azo dye is tested.

1. Introduction

During the last three decades the interest in finding or/ and synthesizing of new materials exhibiting nonlinear optical properties such as having large nonlinear refractive indexes and fast response times grew almost exponentially. Such effects are of technological importance for the future use in applications viz., optical limiting, optical delay, optical switching, all-optical modulation, optical phase conjugation, in data storage [1–16], to name a few. To date, vast number of materials has been studied, shows excellent optical properties and proved their abilities use in number of photonic

* Corresponding author.
E-mail address: qusayali64@yahoo.co.in (Q.M.A. Hassan).

https://doi.org/10.1016/j.saa.2021.119487
1386-1425/

applications. Among these materials organic materials are considered as prime one with excellent optical properties owe to their large nonlinearities which were studied by the present authors during the last four years [17–36].

Change of index of refraction as a result of the passage of a laser beam through a medium can lead to number of nonlinear phenomena in the spatial domain viz., self-phase modulation (SPM), self-focusing, self-defocusing, self-diffraction, optical bi-stability, etc. [37]. Due to the SPM, concentric diffraction ring pattern distributions can be induced on a screen in the far-field post the beam traversing the nonlinear medium.

The changes of refractive index induced by the laser light usually written as follows:

$$n = n_o + n_2 I \quad (1)$$

where n_0 is the linear refractive index of the medium, n_2 is the nonlinear index of refraction and I is the laser light intensity. Based on the number of rings resulted in the diffraction ring patterns technique, the total change in the medium refractive index, Δn, and n_2 can be determined. The Z-scan is another technique which is simple, versatile and effective in determining n_2, the nonlinear absorption coefficient, β, the magnitude of the real and imaginary parts of the nonlinear susceptibility and the sign of n_2 and of real part of the susceptibility.

Sulphanilamide and its derivatives were studied for various reasons since 1965, viz., in the study of the crystal structure of α-sulphanilamide [38], its effect on ^{13}C fluxes [39], its biological evaluation [40], its antibacterial activity [41], its antibiotics to soil organic sorbents [42], its bioglogical screening [43], the spectral study of chelating [44], its antimicrobial activity [45], its pharmacological screening [46], its pharmacological evolution [47], its antimicrobial drugs [48], its spectroscopic, antimicrobial and antioxidant activities [49] etc.

Benzoylacetone and its derivatives have been studied extensively too, viz., toxicity studies [50], tautomery and acid properties [51], synergistic extraction equilibrium of lanthanide (III) ions [52], spectrophotometric study [53], as building block in heterocyclic synthesis [54], etc.

In addition to the fact that azo dyes are widely used in the manufacturing of dyes and textiles, azo compounds are of great importance in many industrial, pharmaceutical, and other fields [55–57]. In the pharmaceutical field, there are a lot of researches indicating the use of azo compounds in the preparation of antipyretic [58], anti-inflammatory [59], anti-tumor [60,61] and anti-bacterial agents [62].

Azo (—N═N—) chromophore group conjugated with aromatic or heterocyclic substitutes that formed azo compounds. The π electron delocalization on the acceptor - donor units across the azo

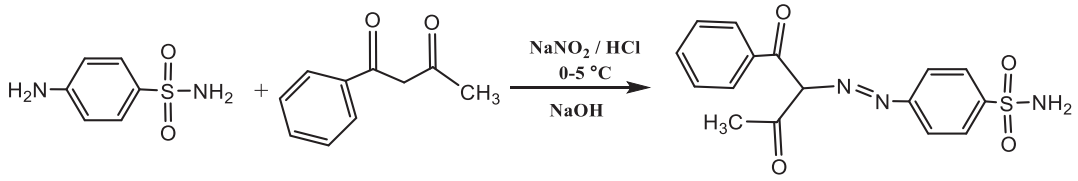

Fig. 1. Synthetic route of azo compound NA4.

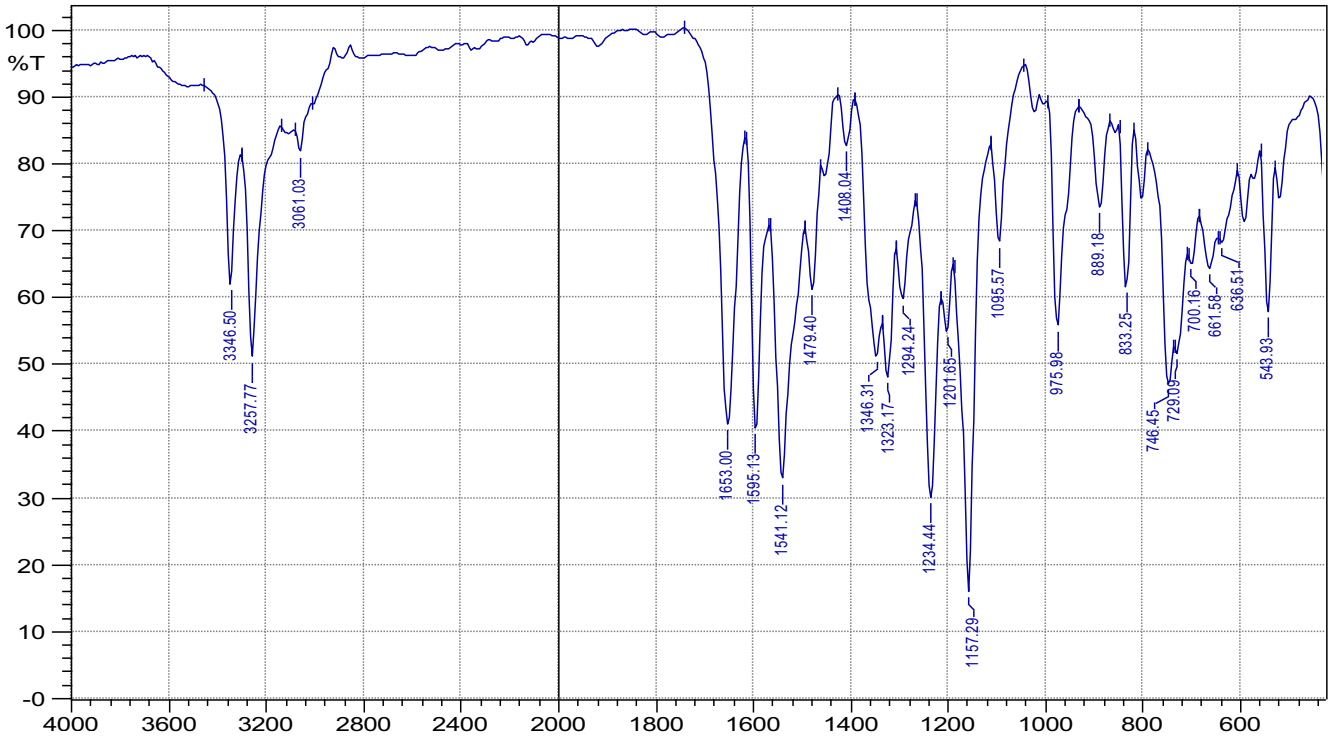

Fig. 2. FTIR spectrum of 4-((1,3-dioxo-1-phenylbutan-2-yl)diazenyl) benzenesulfonamide.

linkage and reorganization of electronic density make this type of compounds exhibited excellent photophysical properties [63]. Anisotropy properties and photoresponsive behavior of azobenzenes compounds made these compounds broadly interesting, Therefore, there are many applications of azobenzenes compounds in areas such as nonlinear optical (NLO) devices, optical switching and liquid crystal displays (LC) [64–66]. Quantum mechanical computations investigations have given useful guidelines in the NLO properties study of organic materials [67].

The main objective of the current study is to find a new material that can be used as an optical limiter for continuous wave (CW) laser beams in low power regime. In this work new material is synthesized for the first time, which is 4-((1,3-dioxo-1-phenylbutan-2-yl) benzensulfonamide by the interaction of sulfanilamide and benzoylacetone. The new material nonlinear properties viz., the nonlinear refractive index and the nonlinear absorption coefficient have been obtained via the diffraction ring patterns and Z-scan techniques using a CW laser beam of wavelength 473 nm.

2. Experimental

2.1. Instrumentation

All the chemicals were used as received without further purification except for aniline, was distilled before use. FT-IR spectrum of the prepared compound was obtained in the range 4000–500 cm^{-1} using KBr disc on Shimadzu FT-IR 8400S spectrometer. ^1H NMR spectrum was recorded on Bruker 500 spectrometer using TMS as an internal reference and DMSOd_6 as a solvent. Mass spectrum for the compound was recorded on Agilent Technologies-5975C (EI, 70 eV).

2.2. Synthesis

2.2.1. Synthesis of the azo compound NA4

The first step sulfanilamide (1.2 g, 0.007 mmol) was dissolved in a 10 mL of distilled water containing 1.5 mL of HCl (36%), the solution was cooled to 0–5 °C in an ice-bath and kept at this temperature. The second step the sodium nitrite solution (0.6 g, 10 mmol) in 5 mL of distilled water was prepared, and added dropwise to the solution obtained from the first step with stirring for 10 min at the same temperature. The obtained diazonium salt solution was added portion wise to the solution of benzoylacetone (1.135 g, 0.007 mol) in 10 mL of ethanol and the corresponding azo compound NA4 precipitated, then dried. The synthesis of the azo compound NA4 is displayed in Fig. 1.

2.2.2. 4-((1,3-dioxo-1-phenylbutan-2-yl)diazenyl) benzenesulfonamide (NA4)

Orange powder. Yield: 70%. m.p.: 198–200 °C. FT-IR (KBr, ν, cm^{-1}): 3346 (N—H), 3061 (C—H Ar.), 2900 (C—H Aliph.), 1653 (C=O), 1636 (C=C), 1479 (N=N), 1323 (C—N). ^1H NMR (500 MHz, DMSO d_6) δ 11.25 (s, 2H), 7.78 (dd, J = 25.4, 8.4 Hz, 2H), 7.56 (t, J = 7.7 Hz, 2H), 7.48 (d, J = 8.5 Hz, 2H), 7.24 (m, 1H), 2.52 (s, 3H). MS (EI, m/z (%)): 345 (M+, 106). UV/Vis λ_{max} (nm): 360 (N=N); 300 (C=O); 250 (Ar-CN).

FTIR, Mass and 1HNMR spectra of prepared azo compound are shown in Figs. 2–4.

2.3. Characterization method

A 10 mM concentration of NA4 solution was prepared by dissolving the NA4 compound in an ethanol solvent. UV–visible spec-

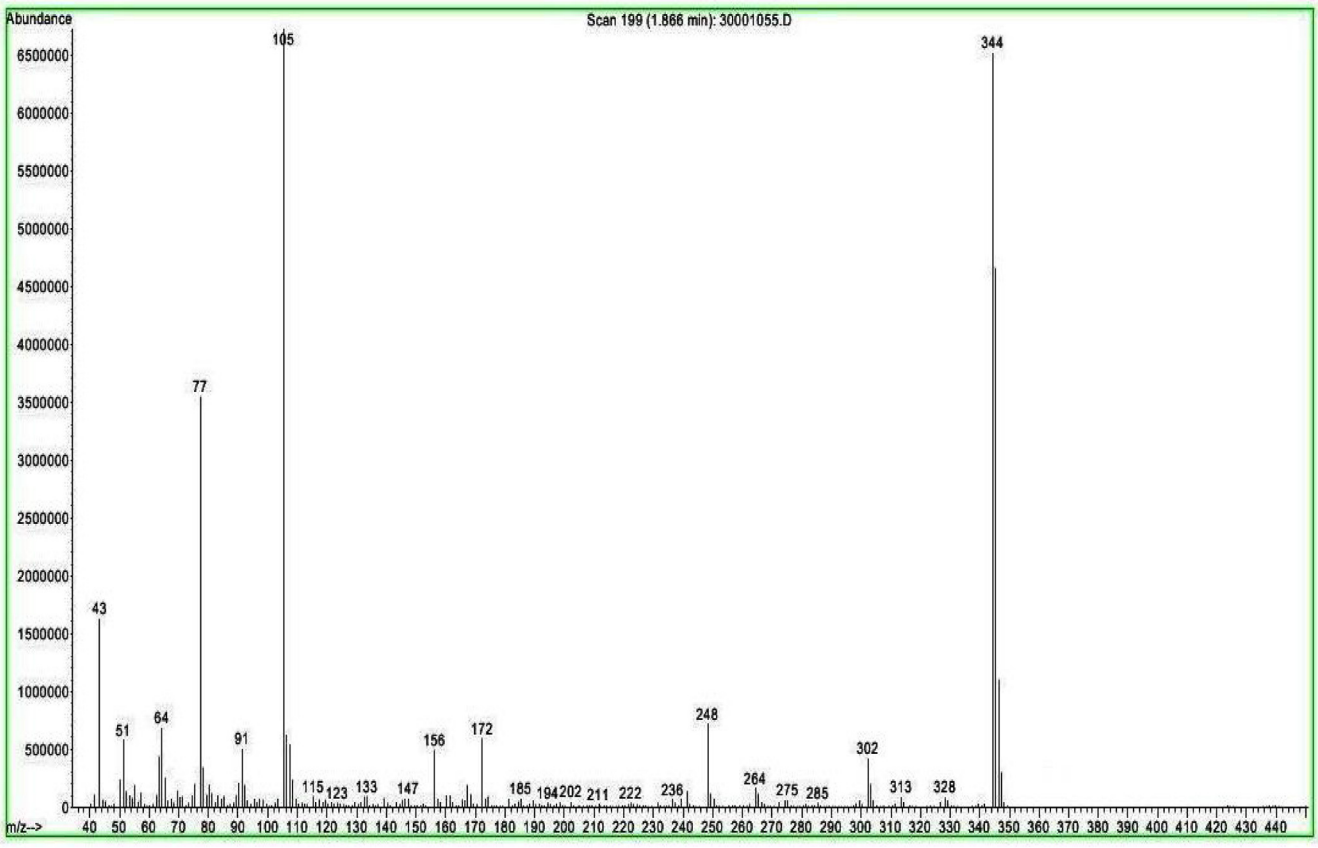

Fig. 3. Mass spectrum of 4-((1,3-dioxo-1-phenylbutan-2-yl)diazenyl) benzenesulfonamide.

trophotometer (PD-303 Japan) was used to measure the absorbance, A, spectrum of the NA4 compound solution placed in a quartz cell with thickness d = 1 mm, at room temperature. Fig. 5 displays the absorbance, A, spectrum of the NA4 compound solution. UV–visible absorbance of group (N=N) in azo compound is given in range 350–370 nm [68]. The prepared azo compound showed an absorption at 360 nm. The UV–visible spectrum also shows a second absorption close to 300 nm due to the carbonyl

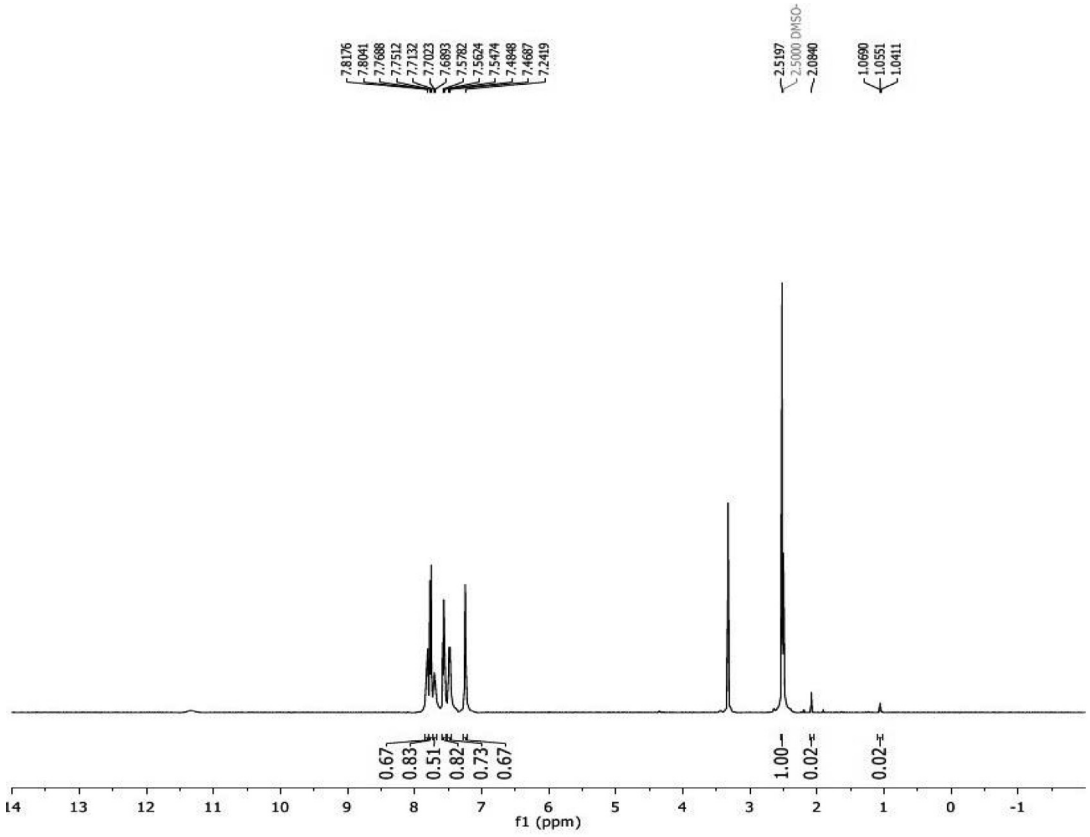

Fig. 4. ^{1}H NMR spectrum of 4-((1,3-dioxo-1-phenylbutan-2-yl)diazenyl) benzenesulfonamide.

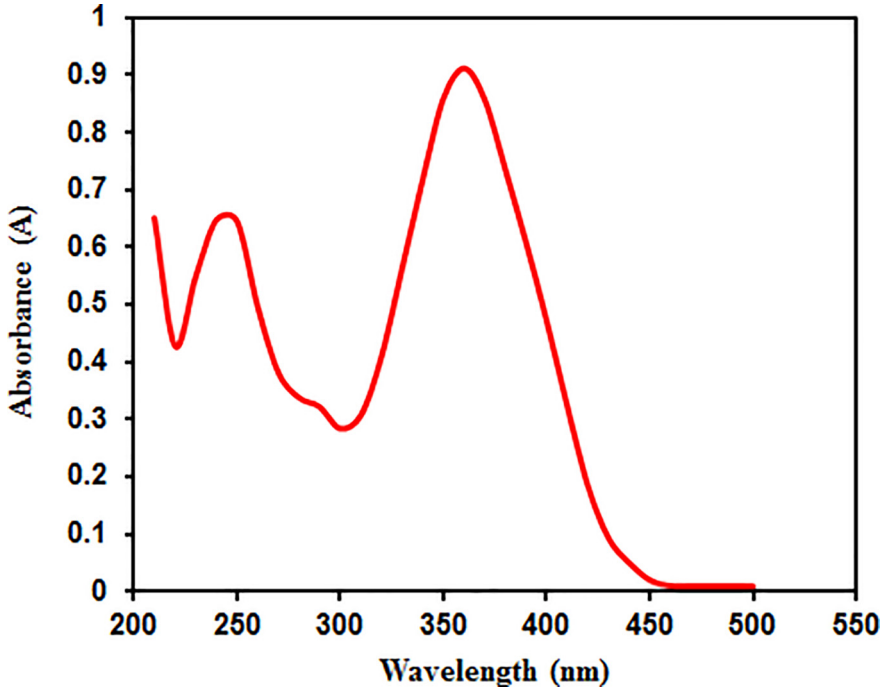

Fig. 5. NA4 compound solution absorbance (A) spectrum.

group (C═O) as a result of the transfer n - π*. Another absorption at 250 nm is caused by the transition of π – π* due to the presence of an aromatic ring and Ar-CN group [69].

By finding the absorbance, A , value of the NA4 compound solution from the Fig. 5 at the wavelength 473 nm and using Eq. (2) [70], we found that the value of the linear absorption coefficient, α, equals 0.207 cm^{-1}.

$$\alpha = 2.303\frac{A}{d} \quad (2)$$

The UV–visible spectrum of synthesized azo dye NA4 compound was calculated using TD-DFT with B3LYP/6-31G(d,p) level. According to the results of the UV–visible spectrum, there are bands in the visible range. The calculated theoretical main bands of NA4 compound came at 355.51, 300.82 and 294 nm respectively,

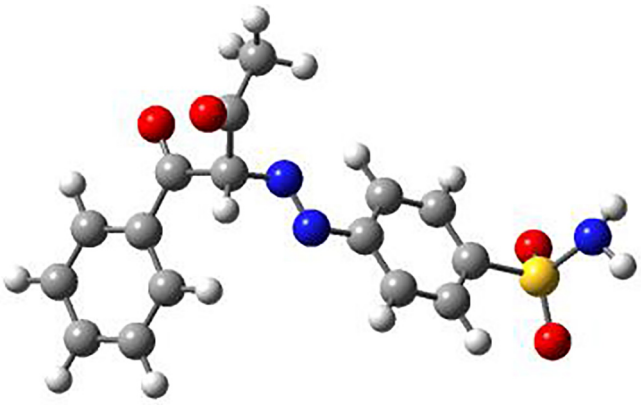

Fig. 7. Optimized structure of azo compound NA4.

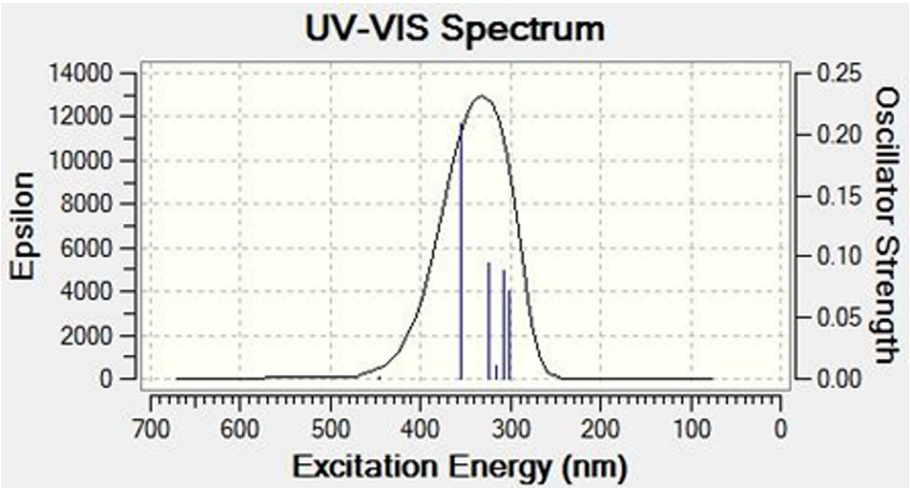

Fig. 6. UV–visible spectrum of NA4 compound calculated by TD-DFT/B3LYP 6-31G(d,p).

Table 1
Excited states of NA4 calculated using TD-DFT with B3LYP/ 6-31G(d,p).

Excited states* (HOMO → LUMO)	State	Percentage contribution (%)	Energy (eV)	Calculated		Exp.
				λmax (nm)	f	
89 → 91	1	38.4	2.7763	446.58	0.001	
90 → 91		57.1				
84 → 91	2	18.7	3.4875	355.51	0.209	360
84 → 92		14.8				
86 → 91		11.8				
89 → 91		51.1				
89 → 92		16.1				
84 → 91	3	20.3	3.8306	323.67	0.094	
84 → 92		17.0				
86 → 91		44.1				
86 → 92		13.2				
87 → 91		11.3				
89 → 91		23.4				
89 → 92		26.9				
87 → 91	4	15.0	3.9236	316.00	0.010	
88 → 91		68.4				
87 → 91	5	21.8	4.1216	300.82	0.072	300
89 → 91		10.0				
89 → 92		25.8				
90 → 92		59.3				
85 → 91	6	55.2	4.2087	294.59	0.0718	250
86 → 91		19.5				
89 → 92		29.7				
90 → 92		12.2				

NA4*, HOMO = 90, LUMO = 91.

Table 2
Observed and calculated vibrational frequencies and relative intensities of NA4 compound.

Obsd.		Calcd.[a]		Obsd.		Calcd.[a]	
υ (cm^{-1})	Int.[b]	υ (cm^{-1})	Int.[c]	υ (cm^{-1})	Int.[b]	υ (cm^{-1})	Int.[c]
3346	m	3412	41.4	1323	m	1319	39.1
3257	m	3300	56.1	1294	w	1311	100
3061	vw	3014	16.3	1234	s	1236	100
2900	s	2914	11.9	1201	m	1212	47.7
1653	s	1656	100	1157	vs	1141	100
1595	s	1587	28.6	1095	m	1090	31.3
1479	w	1484	15.2	975	s	965	99.8
1346	m	1343	100				

[a] Calculated at the DFT/B3LYP/6-31G level scaling 0.94 is used.
[b] Very strong (vs), strong (s), medium (m), weak (w) and very weak (vw) intensities.
[c] Relative intensities.

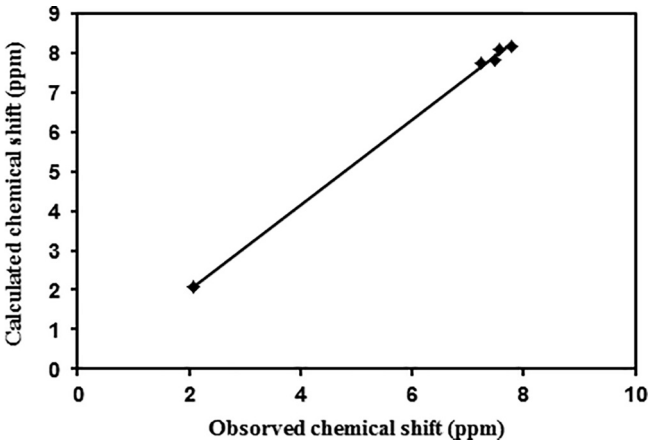

Fig. 8. Plot of the observed vs. the calculated ^{1}H NMR chemical shift of NA4 compound.

as shown in Fig. 6, while the experimentally measured UV–visible spectrum showed values at 360, 300 and 250 nm as shown in Fig. 5. Excited states of synthesized azo dye NA4 compound were determined by TD-DFT/B3LYP 6-31G(d,p) are given in Table 1.

2.4. Experimental setups

The laser beam used in the set of experiments was obtained from a solid state laser device at 473 nm wavelength, CW with single fundamental, TEM_{00}, mode and spot size of 1.5 mm (at $1/e^2$) and output varies from zero to 66 mW. A glass 1 mm thickness sample cell 40 cm away from the laser device output coupler. To focus the laser beam onto the sample cell a glass positive lens of 50 mm focal length was used. The resulted diffraction ring patterns were casted onto a semitransparent 30x30 cm screen, 85 cm from the exit plane of the sample cell. Setup can be seen elsewhere [22].

The Z-scan measurements were conducted using the same setup previously detailed [22], with the screen replaced by a power meter and a circular aperture of 2 mm diameter while the sample cell usually sweeped, by fixing it on a translation stage, across the lens focal point (z = 0) between (−z) and (+z). Such a set-up is the closed aperture, CA, Z-scan. By removing the circular aperture and replaced it with another glass positive lens to collect the entire beam passing through the sample cell, an open aperture, OA, Z-scan is obtained.

The optical limiting property of the sample was obtained using the same set-up used before and fixing the sample at the valley position of the closed aperture Z-scan curve i.e. behind the focal point of the positive lens and using a power meter to measure the output beam power post traversing the sample cell against the variation of input power.

2.5. Computational details

All computations were performed using the Gaussian 09 [71] software package. Full geometry optimizations were performed using the Density Function Theory (DFT) at B3LYP by the 6-31G (d,p) basis set level. Fig. 7 shows the optimized structure of the prepared NA4 azo compound.

2.5.1. Vibrational spectra

The band of N-H stretching vibration coupled doublet at 3346 cm^{-1} and 3257 cm^{-1} due to the asymmetric and symmetric stretching respectively in primary amine. Absorption of C═O at lower wavenumbers (1653 cm^{-1}) due to delocalization of the π electrons of C═O with aromatic C═C, thus reduces the double-bond character.

The observed and calculated infrared spectra and the relative intensities of synthesized azo dye NA4 are listed in Table 2. The theoretical vibrational frequency spectra of NA4 calculated using DFT by the B3LYP at the 6-31G(d,p) basis set level. The scaling factors 0.94 was used in the calculation of stretching frequencies modes. The scaled calculated frequencies [72], show good agreement with the experimental data.

Table 3
Some calculated quantum chemical descriptors of synthesized dye NA4 and urea.

Comps.	E_{HOMO} (eV)	E_{LUMO} (eV)	Ionization potential IE (eV) ($-E_{HOMO}$)	Electron affinity EA (eV) ($-E_{LUMO}$)	E_{gap} (E_{LUMO}-E_{HOMO}) (eV)
NA4	−6.7647	−2.7537	6.7647	2.7537	4.0110
Urea	−6.7587	1.3034	6.7587	−1.3034	8.0621
Comps.	Hardness η(eV) ($\eta = \frac{(IE-EA)}{2}$)	Softness S (eV^{-1}) ($S = \frac{1}{\eta}$)	Optical softness S_o (eV^{-1}) ($S_o = \frac{S}{2}$)	Electron delocalization χ (eV) ($\chi = \frac{(IE+EA)}{2}$)	Chemical potential CP (eV) ($CP = -\chi$)
NA4	2.0055	0.4986	0.2493	4.7592	−4.7592
Urea	4.0310	0.2480	0.1240	2.7276	−2.7276

2.5.2. ^{1}H NMR spectroscopy study

The chemical shift values for ^{1}H MR measurements of NA4 (as shown in Section 2.2.2) shows four different proton environments, which is in agreement with the suggested structure.

The theoretical ^{1}H NMR chemical shift of the prepared compound NA4 have been calculated at B3LYP methods and standard 6-31G (d,p) basis set using the standard GIAO (Gauge-Independent Atomic Orbital) approach [73]. The calculated values are compared with the observed data. A good linear relationship with $r^2 = 0.999$, between the observed and calculated data has been obtained as shown in Fig. 8.

2.5.3. Orbital energies of the molecule NA4

Highest occupied molecular orbital energy (E_{HOMO}) represents the ability to donate an electron, while lowest unoccupied molecular orbital energy (E_{LUMO}) as an electron acceptor represents the

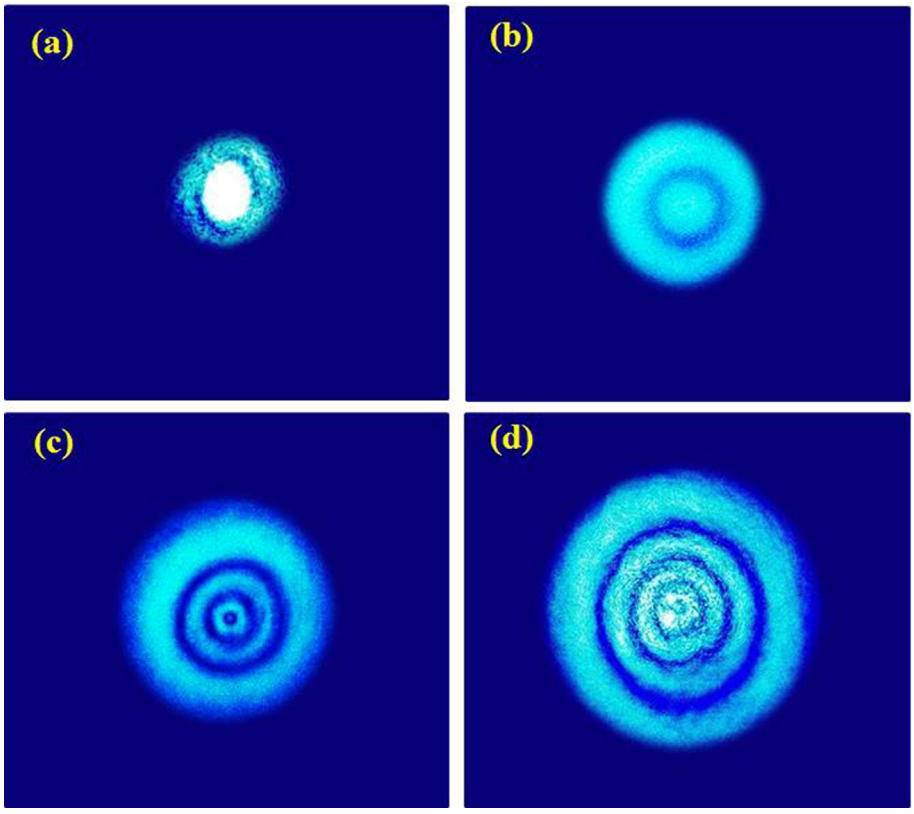

Fig. 9. Diffraction ring patterns appears in NA4 compound solution at input laser beam power (mW): (a) 10 (b) 30 (c) 44 (d) 59.

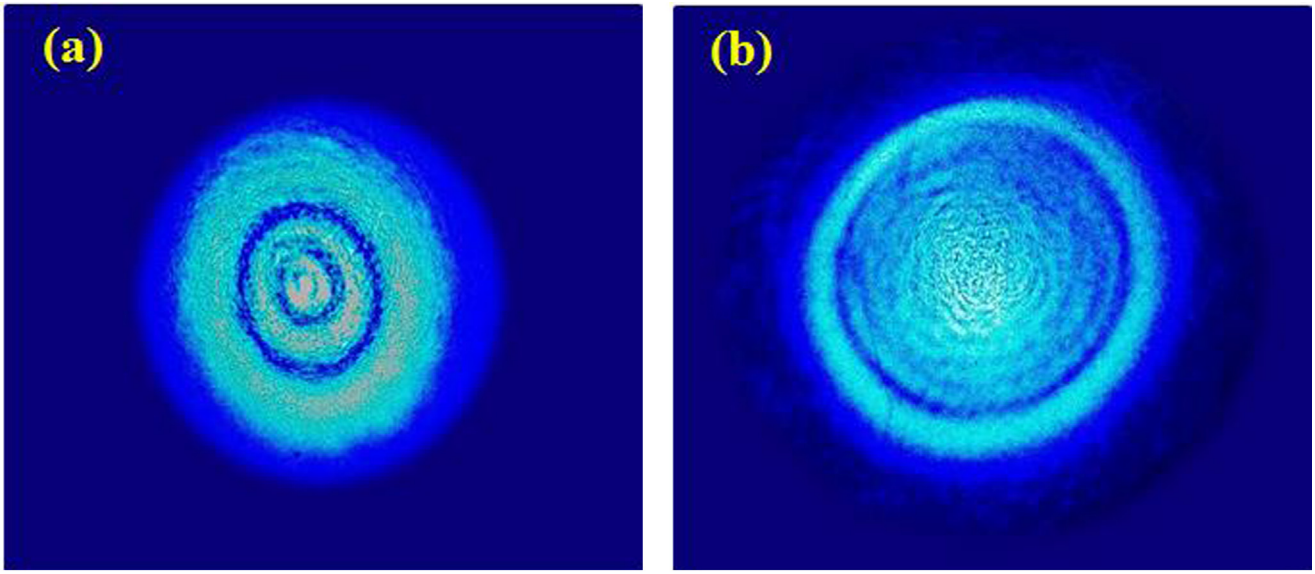

Fig. 10. Diffraction ring patterns in the NA4 compound solution where the laser beam wave front is (a) convergent, (b) divergent at input power of 59 mW.

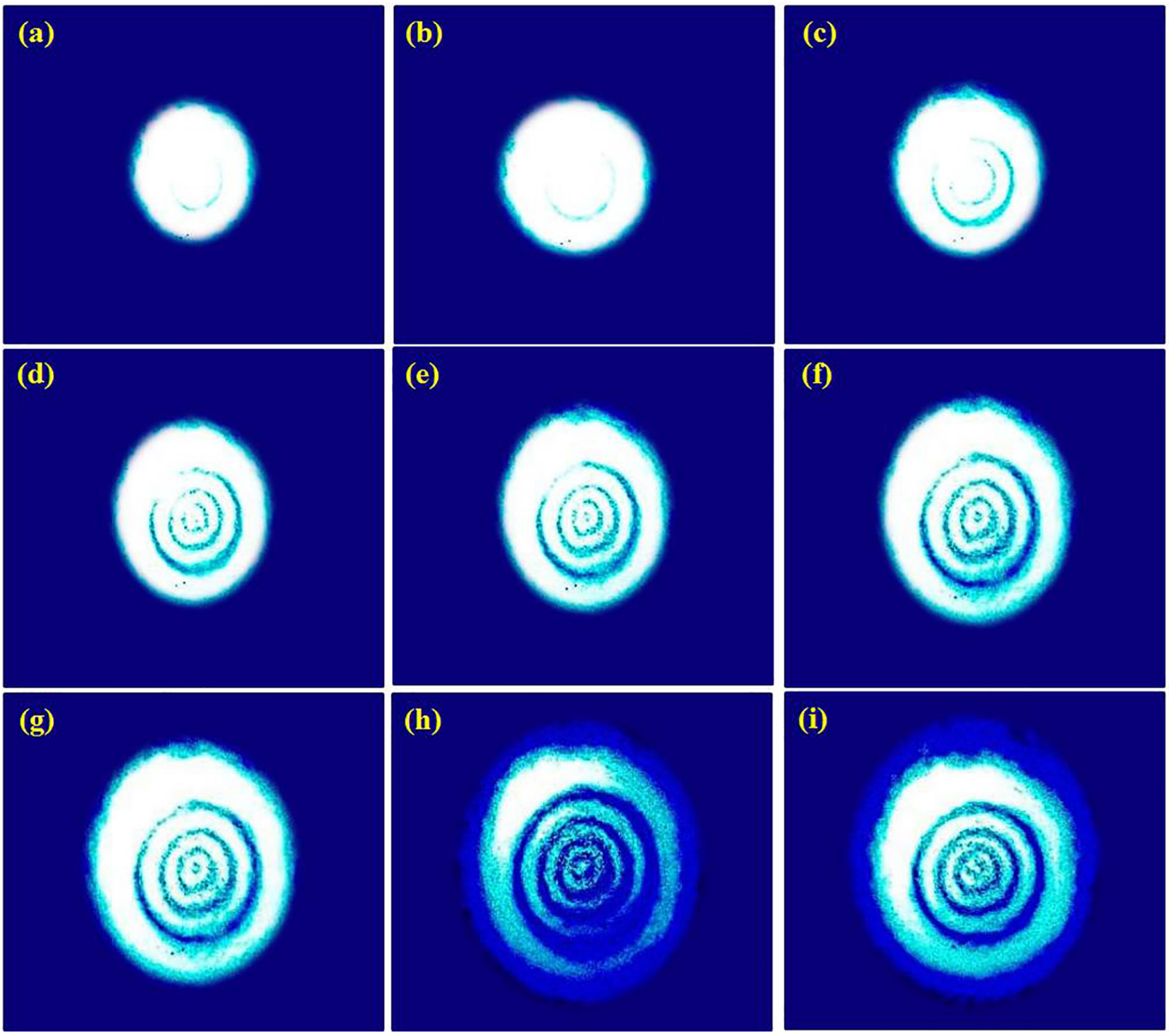

Fig. 11. Temporal development of a chosen diffraction ring pattern in NA4 compound solution at input power of 59 mW: (a) 100 msec (b) 200 msec (c) 300 msec (d) 400 msec (e) 500 msec (f) 600 msec (g) 700 msec (h) 800 msec (i) 1000 msec.

ability to obtain an electron. The HOMO-LUMO energy calculations of the prepared compound were performed using DFT/B3LYP method with 6-31G(d,p) basis set. The energy of the HOMO and LUMO are identified via the ionization potential and the electron affinity respectively [74].

2.5.4. Theoretical investigations of the optical nonlinear (NLO) properties

Nonlinear optical properties of the NA4 compound were investigated theoretically by the calculation of some quantum chemical descriptors, QCDs, using the DFT/B3LYP method with a 6-31G(d,p) basis set in comparison with urea as a standard. The urea is generally used as a reference in the investigations of NLO properties [75], therefore, QCDs, of urea are calculated at the same method and level.

NLO properties of any compound increases according to increasing of E_{HOMO}, softness means (S) and optical softness (S_o). The decreasing of E_{LUMO}, energy gap, ionization potential IE and Hardness (η) means increasing of NLO properties. The results are summarized in Tables 3. The LUMO energy, E_{gap} and hardness of synthesized dye NA4 are −2.7537 eV, 4.0110 eV and 2.0055 eV respectively were less than their values in urea, where they are 1.3034 eV, 8.0621 eV and 4.0310 eV respectively. The softness and optical softness values of prepared compound NA4 are 0.4986 eV^{-1} and 0.2493 eV^{-1} respectively, where they are higher than their values in urea, i.e. 0.2480 eV^{-1} and 0.1240 eV^{-1} respectively. These results indicate that the synthesized dye NA4 have high NLO property than urea.

3. Result and discussion

3.1. Diffraction ring patterns

Fig. 9 represents the dependence of the ring patterns on the input power of the laser beam at wavelength 473 nm traversed the NA4 compound solution in the 1 mm thickness glass cell. Based on the Fig. 9, the number of diffraction rings increase with the increase of input power since absorbed energy increases and more heat resulted. At the same time the ring patterns appears

circular symmetric at low input power when the conduction current that occurs horizontally equals to the vertical convection current. At higher input power vertical convection current exceeds the conduction current that leads to asymmetries of the ring patterns i.e., the upper part of the patterns grew in low ratio compare to lower part where the upper hot layer moves upward and replaced by a cool one i.e. refractive index change is lower than the lower part layer. As the input power increase so does the area of each pattern also the outer most rings in each pattern appear intense compare to the inner ones as a result of self-defocusing. The dependence of type of ring patterns on the laser beam wave front, convergent and divergent, when the sample was 1 cm before and 1 cm after the lens focal point respectively are shown in Fig. 10. The temporal evolution of a chosen ring pattern are shown in Fig. 11, where it can be seen that the ring patterns evolve temporally i.e., appear small and circular at zero sec time then its area increases, the number of rings increases with time and each pattern appear asymmetric as time laps.

3.2. Modeling the diffraction ring patterns:

To qualitatively and quantitatively calculate the diffraction ring patterns obtained in Figs. 9–11, suppose a CW laser beam with Gaussian distribution propagate horizontally along the z- direction and its field vary in the x-y plane from peak power, P, to zero away from the z-direction by a distance $r = (x^2 + y^2)^{1/2}$ where the beam radius ω = rwhen the beam intensity, I, reduced from I_o to I_o/e^2. Let R be the beam wavefront radius, $k = 2\pi/\lambda$, is the laser beam wave vector and λ is the beam wavelength, the laser beam complex field amplitude, $U(x, y, t, z = 0)$, at the entrance of the nonlinear medium can be written as follows [55,76]:

$$U(x, y, t, z = 0) = \left(\frac{2P}{\pi\omega^2}\right)^{1/2} \exp\left(-\frac{r^2}{\omega^2}\right)\exp(-ik\frac{r^2}{2R}) \quad (3)$$

As the beam traverses the nonlinear medium, part of it's energy is absorbed and heat appear as a result of the nonradiative transitions and conduction current appear horizontally in the shape of

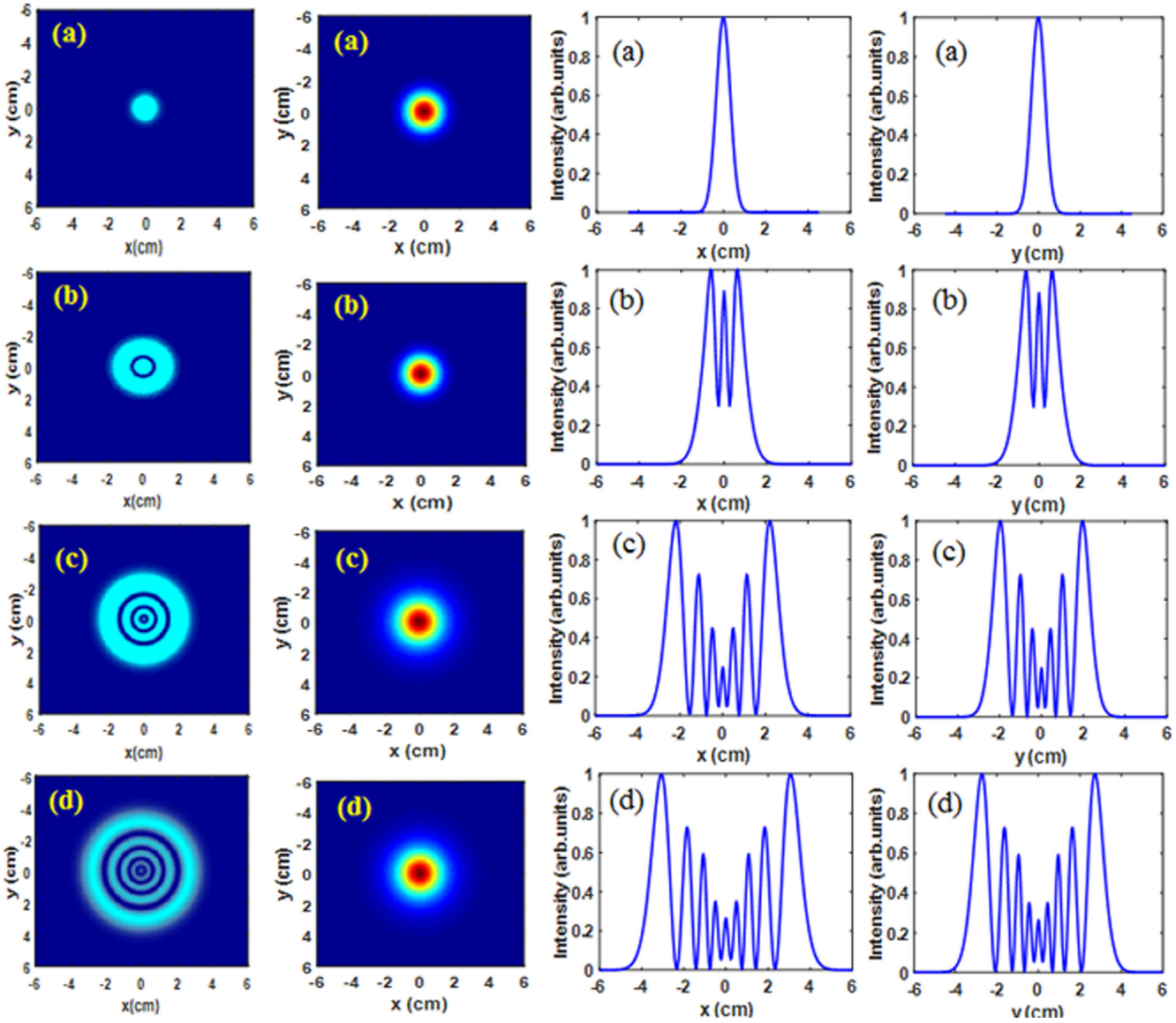

Fig. 12. Simulation results (from left to right columns) of diffraction ring patterns in NA4 compound solution (1st), spatial distributions of laser beam phase (2nd), intensity distributions of laser beam in one dimension (x-3rd) and (y-4th) at power input (mW): (a) 10 (b) 30 (c) 44 (d) 59.

Gaussian distribution. The ring patterns shown in Fig. 9 loses symmetry in the vertical direction suggesting a convection occur in that direction. The asymmetries in the ring patterns increase as time laps and as input power increases too. This supposing a convective velocity, v_x, which can be written as follows [76]:

$$v_x = \frac{\beta g[\Delta T]_{max}\pi h^2}{16\mu} \tag{4}$$

β is the medium thermal expansion, g is the gravity acceleration, h is the distance from the center of the beam to a position at which convection still occur, $[\Delta T]_{max}$ is the maximum change in the nonlinear medium temperature and μ is the medium viscosity.ΔT can be written as follows [76]:

$$\Delta T(x,y,t) = \frac{\alpha p}{\pi\rho C_p}\{\int_0^t \frac{dt'}{8Dt' + \omega^2}\exp(-2[(x - v_x')^2 + y^2]/[8Dt' + \omega^2])\} \tag{5}$$

with $D \approx K/\rho c_p$ is the medium thermal diffusivity and K, ρ, c_p are its thermal conductivity, density and specific heat respectively. The temperature variation lead to variation of the medium refractive index, $n(x,y,t)$, can be written as follows [76]:

$$n(x,y,t) = n_0 + \frac{dn}{dT}\Delta T(x,y,t) \tag{6}$$

n_0 is the NA4 compound solution linear refractive index and dn/dTis its thermoptic coefficient. The change in the medium index of refraction, $n(x,y,t)$, leads to a phase change or shift, $\Delta\varphi(x,y,t)$, can be written as follows [76]:

$$\Delta\varphi(x,y,t) = \frac{2\pi}{\lambda}d[n(x,y,t) - n(0,0,t)] \tag{7}$$

Using the definitions previously introduced, the phase shift (Eq. (7)) can be written as follows:

$$\Delta\varphi(x,y,t) = \frac{(\frac{dn}{dT})\alpha PL}{2\lambda k t_c}\int_0^t \frac{dt'}{\left(1 + \frac{2t'}{t_c}\right)}\{\exp(-2[(x - v_x t')^2 + y^2]/[\left(1 + \frac{2t'}{t_c}\right)\omega^2]) - \exp(-2(v_x t')^2/[\left(1 + \frac{2t'}{t_c}\right)\omega^2] \tag{8}$$

The characteristic heat diffusion time $t_c \approx \omega^2/4D$.

The light field complex amplitude, $U(x,y,t,z=0)$, at the exit plane of the nonlinear medium cell can be rewritten as follows [76]:

$$U(x,y,t,z=0) = \left(\frac{2p}{\pi\omega^2}\right)^{\frac{1}{2}}\exp(-\frac{\alpha d}{2}).\exp\left(-ik\frac{x^2+y^2}{\omega^2}\right).\exp\left(-\frac{x^2+y^2}{2R}\right)\exp(i\Delta\varphi(x,y,t)) \tag{9}$$

The intensity distribution of laser beam, $I(x',y',t)$, on the screen in the far field with respect to a distance F away from the sample cell exist plane where the spatial coordinates are rewritten as (x',y'), using the Fresnel-Kirchhoff theory and Franuhofer approximation can be written as follows [76]:

$$I(x',y',t) = |\left(\frac{2P}{\pi\omega^2}\right)^{\frac{1}{2}}\frac{i\pi\omega^2}{\lambda F}\exp(ikF)\exp\left(-\frac{\alpha d}{2}\right)\int_{-\infty}^{\infty}dx \times \int_{-\infty}^{\infty}dy.\exp\left(-\frac{x^2+y^2}{\omega^2}\right).\exp[i\left(-k\frac{x^2+y^2}{2R}\right) + \Delta\varphi(x,y,t)].\exp\left(-ik\frac{xx'+yy'}{F}\right)|^2 \tag{10}$$

Eq. (10) was solved numerically using the MATLAB system. Figs. 12–14 are the simulation results based on the solution of Eq. (10). Results of Fig. 12 can be well compared with those given in Fig. 9 for the diffraction ring pattern evolution as input power increase. Fig. 13 shows the type of ring patterns dependence on the the laser beam wave front type which can be compared with those shown in Fig. 10. Fig. 14 shows the temporal evolution of a chosen ring pattern which can be compared with those given in Fig. 11. The overall simulation results agree well with those measured.

3.3. Diffraction ring pattern:

The estimation of the induced total change in the NA4 compound solution index of refraction, Δn, can be carried based on the geometrical optics. When a single ring resulted post the propagation of the laser beam in the NA4 compound solution an indica-

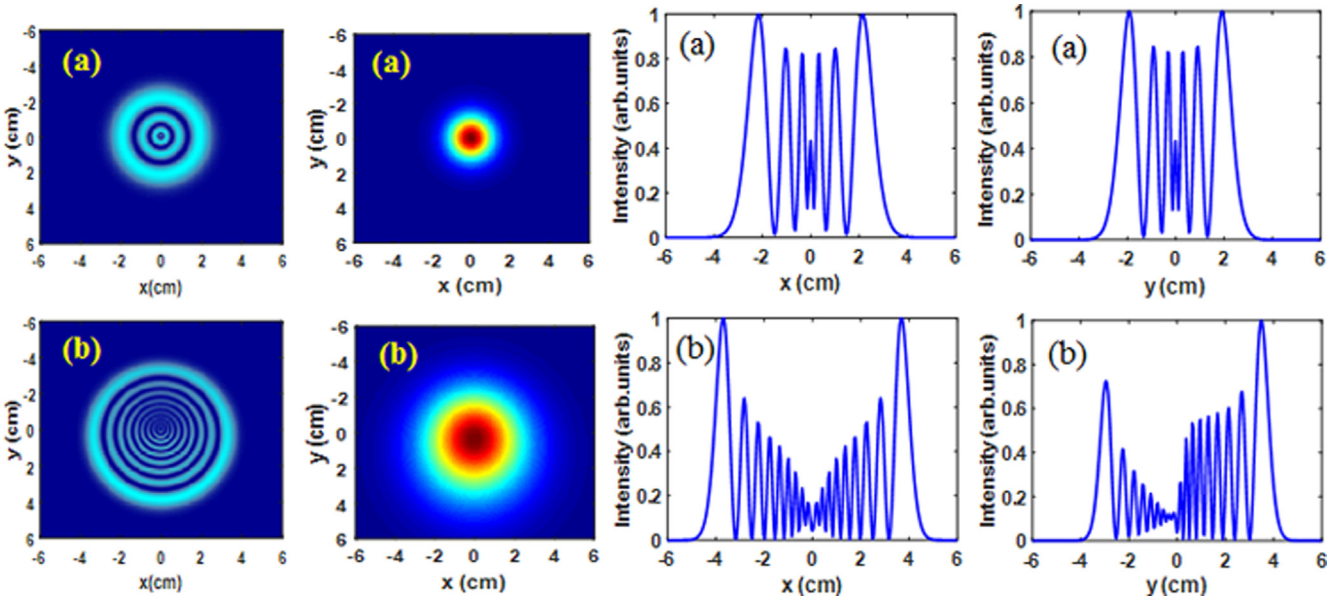

Fig. 13. Simulation results (from left to right columns) diffraction ring patterns in NA4 compound solution (1st), laser beam phase spatial distributions (2nd), 1 dimensional intensity distributions of laser beam (x-3rd) and (y-4th) where the laser beam wave front is convergent (upper row) and divergent (lower row) at input power 59 mW.

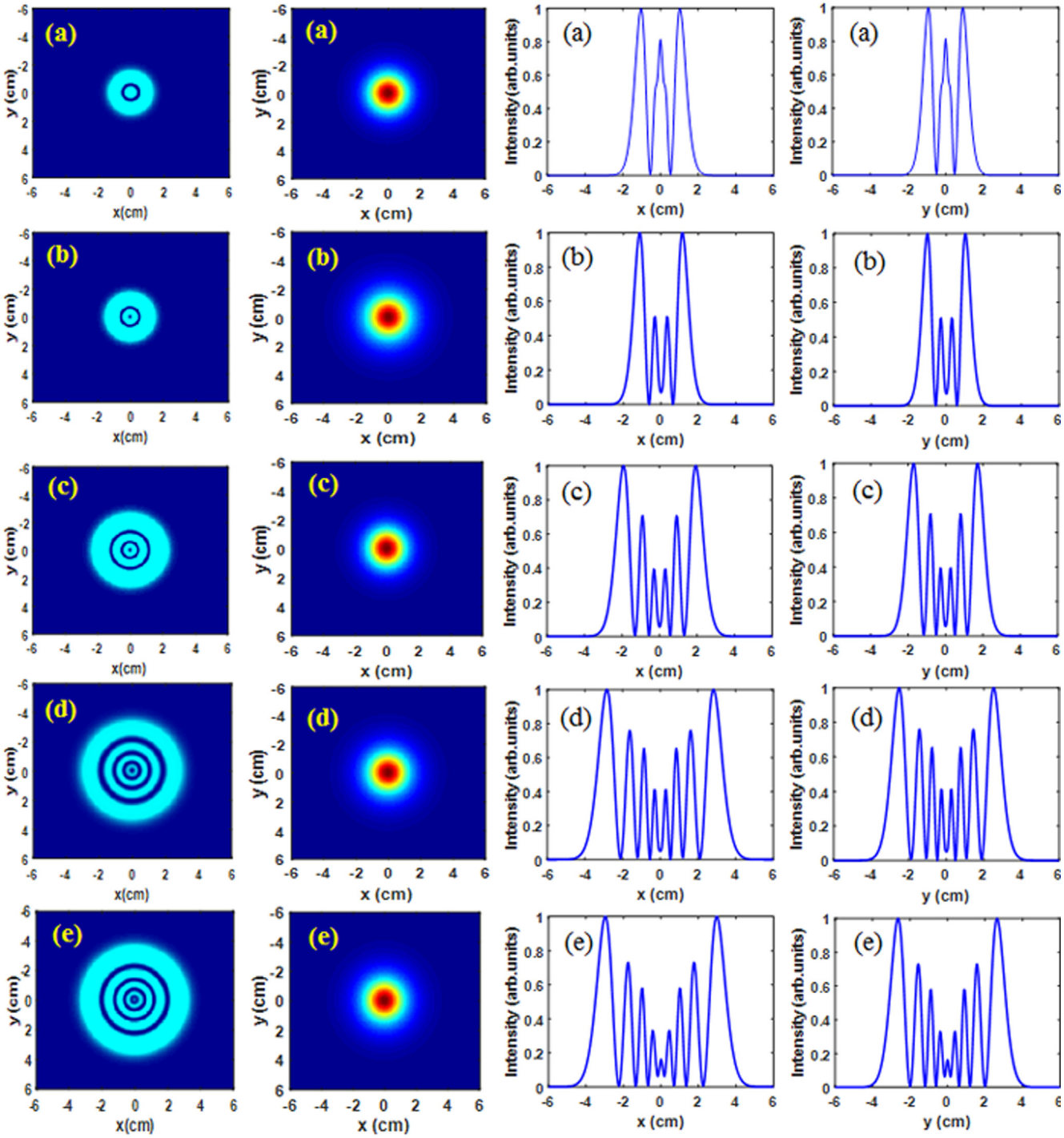

Fig. 14. Simulation results of temporal development (from left to right columns) of the chosen diffraction ring pattern in NA4 compound solution (1st), spatial distributions of the laser beam phase (2nd), 1 dimensional intensity distributions (x-rd) and (y-4th) at input power of 59 mW: (a) 100 msec (b) 200 msec (c) 300 msec (d) 400 msec (e) 500 msec (f) 600 msec (g) 700 msec (h) 800 msec (i) 1000 msec.

tion of a phase change in the laser beam of 2π radians. For total N rings a total phase change in the NA4 compound solution, $\Delta\varphi$, of 2πN radians can be written as [77]

$$\Delta\varphi = 2\pi \mathrm{N} \tag{11}$$

$\Delta\varphi$ can be related to the sample thickness, d, the laser beam wave vector, $k = 2\pi/\lambda$, and Δn as follows:

$$\Delta\varphi = kd\Delta n \tag{12}$$

So that

$$\Delta n = \frac{N\lambda}{d} \tag{13}$$

λ is the laser beam wavelength, and

$$\mathrm{n}_2 = \frac{\Delta \mathrm{n}}{\mathrm{I}} \tag{14}$$

wherel is the laser beam intensity ($=\frac{2P}{\pi\omega^2}$).

For number of rings N, 3, for NA4 compound solution, d = 0.1 cm, beam spot size, ω, of 19.228 μm, λ = 473 nm, laser beam

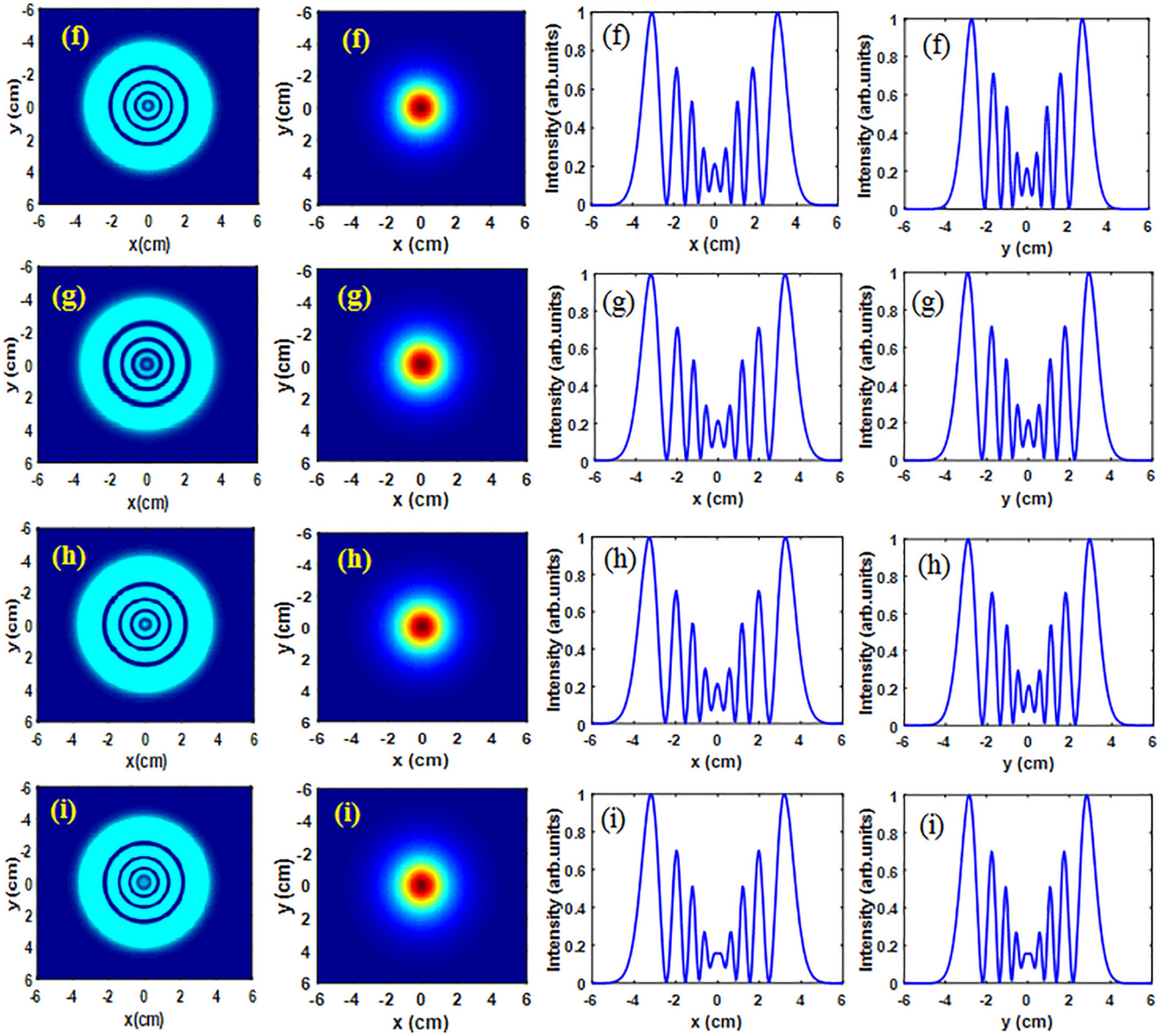

Fig. 14 (*continued*)

intensity = 7408 W/cm^2 so that Δn is equal to 1.419 × 10^{-3} and n_2 equals 1.915 × 10^{-7} cm^2/W.

3.4. Z-scan

In the current study, both types of Z-scans measurements were performed viz., the closed and open aperture Z-scans. Fig. 15 shows the results of the CA Z-scan to the NA4 compound solution. From the Fig. 15, we can conclude that the self-defocusing has occurred to laser beam, which means that the NA4 compound solution has a negative nonlinear index of refraction, because the curve shows a peak followed by a valley. The nonlinearity shown by the NA4 compound solution is thermal due to the use of a CW laser beam, and it results in the formation of a thermal divergence lens due to the energy absorption from the laser beam by the NA4 compound solution, which leads to its heating. This lens induces a phase shift in the laser beam; when the amount of shift is less than 2π radians, self-defocusing set's in, and when the phase shift is ≥ 2π radians a diffraction ring patterns appears.

We obtained a straight line when conducting an OA Z-scan, which indicates that the NA4 compound solution does not have a nonlinear absorption coefficient. This is expected because the measurements were made using a non-resonant wavelength, and at this wavelength a reverse saturation absorption (RSA) or two-photon absorption (TPA) must be obtained when using a pulsed laser, and since a CW beam was used, neither RSA nor TPA can be obtained.

Since the nonlinearity origin exhibited by the sample is thermal, therefore the Cuppo et al., model [78] can be used, so that the nonlinear index of refraction, n_2, can be determined based on the relation [79]

$$n_2 = \frac{\Delta T_{p-v}\lambda}{4\pi I d} \tag{15}$$

ΔT_{p-v} is the difference between the peak and valley transmittances. From Fig. 15 and using the value of T_{p-v} in Eq. (15) with the laser beam intensity = 1721 W/cm^2, we can determine the value of the nonlinear index of refraction of NA4 compound solution and find it is equal to 1.075 × 10^{-8} cm^2/W.

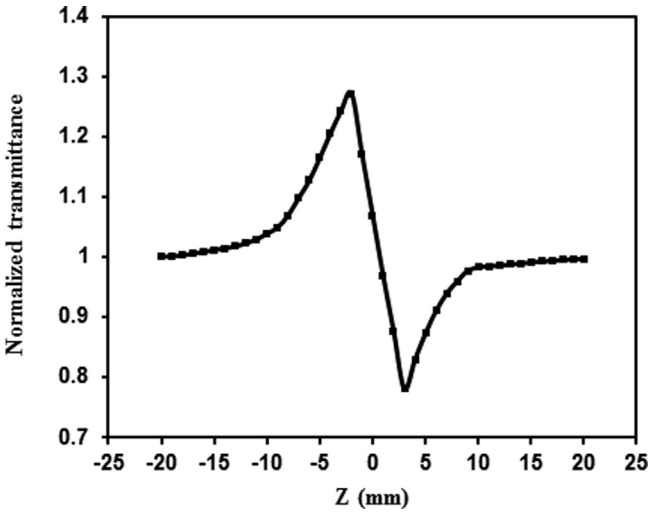

Fig. 15. Experimental results of CA Z-scan measurement of the NA4 compound solution.

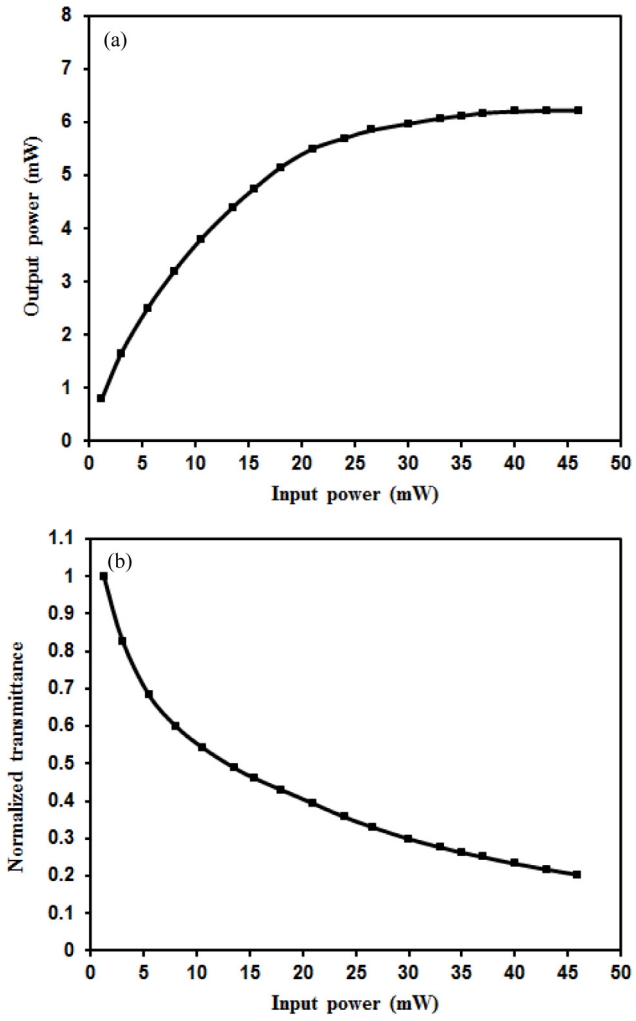

Fig. 16. (a) Experimental results of the optical limiting (b) variation of the normalized transmittance against input power of the NA4 compound solution.

3.5. Optical limiting

After studying the nonlinear optical properties of the NA4 compound solution, it was found that the NA4 compound solution has high nonlinear optical properties represented by the high nonlinear refractive index, which encouraged us to study the properties of the optical limiting of the NA4 compound solution since it possesses high nonlinear optical properties, therefore it is expected to possess the properties of the optical limiting. Fig. 16a depicts the properties of the optical limiting of the NA4 compound solution, where the variation in output power is plotted as a function of input power. As expected, the NA4 compound solution possessed properties of the optical limiting. From Fig. 16a it is noticed that, as the input power is low the output power changes linearly, while at high input power the relation is nonlinear, as the increase of the input power, the output power becomes constant.

After the NA4 compound solution has proved that it possesses the properties of the optical limiting, this is not sufficient for the NA4 compound solution to be used as an optical limiter. To determine the use of the NA4 compound solution as an optical limiter, the limiting threshold, T_H, must be obtained, which represents the value of the input power for which transmittance through the sample is reduced to halve. Plotting the transmittance as a function of the input power is shown in Fig. 16b, from which we find that the value of T_H of NA4 compound solution is 12.4 mW.

3.6. Comparative study

When comparing the nonlinear index of refraction value of a NA4 compound solution computed by the diffraction ring patterns and Z-scan methods, we find that its value calculated by the former method is greater than the latter one for the NA4 compound solution. The reason for this is that the refractive index depends on the incident intensity, and the intensity used in the diffraction ring patterns method is greater than the intensity used in the Z-scan method. Therefore, the value of the nonlinear index of refraction by the former method is greater than its value calculated by the latter method.

Post comparing the nonlinear index of refraction value of the NA4 compound solution computed by two methods, we will in this paragraph compare the nonlinear index of refraction value of the NA4 compound solution computed by Z-scan with its values of other materials [80–83], and it is worth noting here that in these studies [80–83], the Z-scan method and cw laser were used. From comparison, we find that the value of the nonlinear index of refraction of the materials mentioned in these studies [80–83], are less than that of the NA4 compound solution, which confirms that the NA4 compound solution can be used in optical applications.

Now we will compare the threshold value of a NA4 compound solution with its values for the materials mentioned in Refs. [84–87] as these materials were known to have threshold values suitable for being candidates for use as optical limiters. It must be pointed out again that a cw laser beam was used when studying the properties of the optical limiting for the materials mentioned in Refs. [84–87]. As a result of this comparison, we can conclude that the value of the threshold limiting for the materials mentioned in Refs. [84–87] are greater than the value of the NA4 compound solution, which indicates that the NA4 compound solution is more efficient than those materials when it is used as an optical limiter.

4. Conclusions

Azo compounds are of widespread interest and applications, so the azo compound 4-((1,3-dioxo-1-phenylbutan-2-yl)diazenyl)benzenesulfonamide was prepared by the coupling reaction of dizonium salt of sulfanilamide with benzoylacetone. The passage of laser beam of low power continuous wave through the azo compound have led to the generation of diffraction ring patterns. Based

on ring patterns and the Z-scan techniques the nonlinear refractive index of the prepared azo compound has been calculated. The use of the Fresnel-Kirchhoff theory and Mat Lab numerical system, have led to the simulation result that agree well with experimentally observed ring patterns. Optical limiting threshold of 12.4 m of the azo dye have been calculated at the 473 nm wavelength. The aim of the current study is achieved by finding a new material that could be a good candidate to be used as optical limiter for CW laser beams in low power regime.

Declaration of Competing Interest

The authors declare that they have no known competing financial interests or personal relationships that could have appeared to influence the work reported in this paper.

References

[1] Qusay M.A. Hassan, R.K.H. Manshad, Surface morphology and optical limiting properties of azure B doped PMMA film, Opt. Mat. 92 (2019) 22–29.
[2] Qusay M.A. Hassan, Two-photon absorption-based optical limiting in 2-(2-methoxybenzyllideneamino)-5-methylphenylmercuric chloride-doped PMMA film, Mod. Phys. Lett. B 28 (2014), 1450079(10 pp).
[3] R.K.H. Manshad, Qusay M.A. Hassan, Optical limiting properties of magenta doped PMMA under CW laser illumination, Adv. Appl. Sci. Res. 3 (2012) 3696–3702.
[4] Qusay M.A. Hassan, R.K.H. Manshad, Optical limiting properties of sudan red B in solution and solid film, Opt. Quant. Electron. 47 (2015) 297–311.
[5] Qusay M.A. Hassan, Study of nonlinear optical properties and optical limiting of acid green 5 in solution and solid film, Opt. Las. Tech. 106 (2018) 366–371.
[6] Qusay M.A. Hassan, Investigation on the nonlinear optical properties and optical power limiting of parsley oil, Int. J. Photo. Opt. Tech. 3 (2017) 17–20.
[7] Qusay M.A. Hassan, Nonlinear optical and optical limiting properties of chicago sky blue 6B doped PVA film at 633nm and 532 nm studied using a continuous wave laser, Mod. Phys. Lett. B 22 (2008) 1589–1597.
[8] R.K.H. Manshad, Qusay M.A. Hassan, Nonlinear characterization of orcein solution and dye doped polymer film for application in optical limiting, J. Bas. Res. 38 (2012) 125–133.
[9] S. Stopinski, M. Malinowski, R. Piramidowicz, E-Kleijn, M.K. Smit, X.J. Leijtens, Integrated optical delay lines for time division multiplexers, IEEE Photo. J. 5 (2013), 7902109(11pp).
[10] M.F. Al-Mudhaffer, A.Y. Al-Ahmad, Qusay M.A. Hassan, C.A. Emshary, Optical characterization and all-optical switching of benzenesulfonamide azo dye, Optik 127 (2016) 1160–1166.
[11] A.T. Pham, L.N. Binh, All-optical modulation and switching using a nonlinear-optical directional coupler, J. Opt. Soc. Am. B 8 (1991) 1914–1931.
[12] Qusay M. Ali, P.K. Palanisamy, Optical phase conjugation by degenerate four-wave mixing in basic green 1 dye-doped gelatin film using He–Ne laser, Opt. Las. Tech. 39 (2007) 1262–1268.
[13] S. Manickasundaram, P. Kannan, R. Kumaran, R. Velu, P. Ramamurthy, Qusay M.A. Hassan, P.K. Palanisamy, S. Senthil, S. Sriman Narayanan, Holographic grating studies in pendant xanthene dyes containing poly (alkyloxymethacrylate)s, J. Mat. Sci: Mat. Electron. 22 (2011) 25–34.
[14] S. Manickasundaram, P. Kannan, Qusay M.A. Hassan, P.K. Palanisamy, Azo dye based poly(alkyloxymethacrylate)s and their spacer effect on optical data storage, J. Mat. Sci: Mat. Electron. 19 (2008) 1045–1053.
[15] S. Manickasundaram, P. Kannan, Qusay M.A. Hassan, P.K. Palanisamy, Holographic grating formation in poly(methacrylate) containing pendant xanthene dyes, Optoelec. Adv. Mat. Rap. Commun. 2 (2008) 324–331.
[16] Qusay M. Ali, P.K. Palanisamy, S. Manickasundaram, P. Kannan, Sudan IV dye based poly(alkyloxymethacrylate)films for optical data storage, Opt. Commun. 267 (2006) 236–243.
[17] S.A. Ali, Qusay M.A. Hassan, C.A. Emshary, H.A. Sultan, Characterizing optical and morphological properties of Eriochrome Black T doped polyvinyl alcohol film, Phys. Scr. 95 (2020), 095814 (11pp).
[18] Bahjat A. Saeed, Qusay M.A. Hassan, C.A. Emshary, H.A. Sultan, Rita S. Elias, The nonlinear optical properties of two dihydropyridones derived from curcumin, Spectrochim. Acta, Part A: Mol. Biomol. Spectrosc. 240 (2020), 118622(14 pp).
[19] Jabbar H. Jebur, Qusay M.A. Hassan, Mohammed F. Al-Mudhaffer, Ahmed S. Al-Asadi, Rita S. Elias, Bahjat A. Saeed, C.A. Emshary, The gamma radiation effect on the surface morphology and optical properties of alphamethyl curcumin: PMMA film, Phys. Scr. 95 (2020), 045804 (10pp).
[20] Rita S. Elias, Qusay M.A. Hassan, C.A. Emshary, H.A. Sultan, Bahjat A. Saeed, Formation and temporal evolution of diffraction ring patterns in a newly prepared dihydropyridone, Spectrochim. Acta Part A: Molec. Biomol. Spec. 223 (2019), 117297(16 pp).
[21] H.A. Sultan, Qusay M.A. Hassan, Ahmed S. Al-Asadi, Rita S. Elias, H. Bakr, Bahjat A. Saeed, C.A. Emshary, Far-field diffraction patterns and optical limiting properties of bisdemethoxycurcumin solution under CW laser illumination, Opt. Mat. 85 (2018) 500–509.
[22] Rita S. Elias, Qusay M.A. Hassan, H.A. Sultan, Ahmed S. Al-Asadi, Bahjat A. Saeed, C.A. Emshary, Thermal nonlinearities for three curcuminoids measured by diffraction ring patterns and Z-scan under visible CW laser illumination, Opt. Las. Tech. 107 (2018) 131–141.
[23] H.A. Sultan, Qusay M.A. Hassan, H. Bakr, Ahmed S. Al-Asadi, D.H. Hashim, C.A. Emshary, Thermal-induced nonlinearities in rose, linseed and chamomile oils using CW visible laser beam, Can. J. Phys. 96 (2018) 157–164.
[24] Amjad F. Abdulkader, Qusay M. Ali Hassan, Ahmed S. Al-Asadi, H. Bakr, H.A. Sultan, C.A. Emshary, Linear, nonlinear and optical limiting properties of carbon black in epoxy resin, Optik 160 (2018) 100–108.
[25] Qusay M.A. Hassan, H.A. Sultan, Ahmed S. Al-Asad, Ayat Jawdat Kadhim, Nazar A. Hussein, C.A. Emshary, Synthesis, characterization, and study of the nonlinear optical properties of two new organic compounds, Synth. Met. 257 (2019), 116158 (14 pp).
[26] Faeza A. Almashal, Mohammed Q. Mohammed, M.A. Qusay, C.A. Hassan, H.A. Sultan Emshary, Adil M. Dhumad, Spectroscopic and thermal nonlinearity study of a Schiff base compound, Opt. Mat. 100 (2020), 109703 (12 pp).
[27] Qusay M.A. Hassan, H.A. Sultan, Ahmed S. Al-Asadi, H. Bakr, D.H. Hashim, C.A. Emshary, Diffraction ring patterns and Z-scan measurements of nonlinear refractive index of khoba vegetable oil, J. Bas. Res. Sci. 44 (2018) 47–63.
[28] Ayat J. Kadhum, Nazar A. Hussein, Qusay M.A. Hassan, H.A. Sultan, Ahmed S. Al-Asadi, C.A. Emshary, Investigating the nonlinear behavior of cobalt (II) phthalocyanine using visible CW laser beam, Optik 157 (2018) 540–550.
[29] Qusay M.A. Hassan, H.A. Sultan, H. Bakr, Isra M. Ali, R.M. Hassan, C.A. Emshary, Estimating the nonlinear refractive index of 10W30 oil using visible low power laser beam, Res. 10 (2018) 46–51.
[30] C.A. Emshary, H.A. Sultan, Qusay M.A. Hassan, H. Bakr, Nonlinearities of a brake fluid using low visible laser beam, Int. J. Phys. Appl. Sci. 6 (2019) 42–53.
[31] Qusay M.A. Hassan, H. Bakr, H.A. Sultan, Raed M. Hassan, C.A. Emshary, Evolution of far-filed diffraction patterns and nonlinear optical properties of SAE 70 oil, Int. J. Appl. Nat. Sci. 6 (2017) 181–188.
[32] Qusay M.A. Hassan, H. Bakr, C.A. Emshary, H.A. Sultan, Studying the surface morphology, optical and nonlinear optical properties of epoxy resin doped nickel nitrate film, Optik 213 (2020), 164771 (9 pp).
[33] Ahmed Majeed Jassem, Qusay M.A. Hassan, C.A. Emshary, H.A. Sultan, Faeza Abdulkareem Almashal, Wisam Abdulhassan Radhi, Synthesis and optical nonlinear properties performance of azonaphthol dye, Phys. Scr. 96 (2021), 025503 (20 pp).
[34] Ahmed S. Al-Asadi, Qusay M.A. Hassan, Amjed F. Abdulkader, Mohammed H. Mohammed, H. Bakr, C.A. Emshary, Formation of graphene nanosheets/epoxy resin composite and study its structural, morphological and nonlinear optical properties, Opt. Mat. 89 (2019) 460–467.
[35] Mahmoud Sh. Hussain, Qusay M.A. Hassan, H.A. Sultan, Ahmed S. Al-Asadi, Hani T. Chayed, C.A. Emshary, Preparation, characterization, and study of the nonlinear optical properties of a new prepared nanoparticles copolymer, Mod. Phys. Lett. B 33 (2019), 1950456 (17 pp).
[36] Ghufran M. Shabeeb, C.A. Emshary, Qusay M.A. Hassan, H.A. Sultan, Investigating the nonlinear optical properties of poly eosin-Y phthalate solution under irradiation with low power visible CW laser light, Phys. B 578 (2020), 411847(13pp).
[37] W.R. Callen, B.G. Huth, R.H. Pantell, Optical patterns of thermally self-defocused light, Appl. Phys. Lett. 11 (1967) 103–105.
[38] B.H. O'connor, E.N. Maslen, The crystal structure of α-sulphanilamide, Act. Cryst. 18 (1965) 363–366.
[39] V. Prabhu, K.B. Chaston, H. Lui, G.D. Abrams, J. King, Effects of sulfamilamide and methotrexate on ^{13}C fluxes through the glycine decarboxylase serine hydroxymethyl transferase enzyme system in arabidopsis, Planet Physoil 116 (1998) 137–144.
[40] I. Agryropoulou, A. Geronikaki, P. Vicini, F. Zain, Synthesis and biological evalution of sulfonamide thiazole and benzothiazole derivatives as antimicrobial agents, ARKIVOC vi (2009) 89–102.
[41] B.B. Subudhi, G. Ghosh, Synthesis and antibacterial activity of some heterocyclic derivatives of sulfanilamide, Bull. Chem. Ethiop. 26 (4) (2012) 55–460.
[42] J. Schwarz, S. Thiele-Bruhn, K.-U. Echardt, H.-R. Schulten, Sorption of sulfonamide antibiotics to soil organic sorbents: batch experiments with mode compounds and computational chemistry, Int. Schol. Res. Net. 195185 (2012) (9 pp).
[43] S.S. Mohamed, A. Abo-Baker, S.M. Bensaber, M.I. Jaeda, T. Almog, Synthesis and biological screening of some new sulfanilamide schiffs bas, Int. J. Pharm. Pharmac. Sci. 5 (3) (2013) 8–40.
[44] B.K. Patel, N.K. Prajapati, D.G. Patel, Synthesis, characterization and spectral study of chelating azo dyes containing salicylic acid ligand, Pel. Res. Lib. 4 (2013) 70–72.
[45] S. Alyar, N. Karacan, Synthesis, characterization, antimicrobial activity and structure- activity relationships of new aryldisulfonamides, J. Enz. Inhib. Medic. Chem. 24 (2009) 988–992.
[46] R.K. Konda, V.K. Nuthakki, Ch.N. Reddy, Synthesis, characterization and pharmacological screening of substituted sulphonamide derivatives, Sch. Aca. J. Pharm. 3 (2014) 344–349.
[47] M.H. Mohammed, M.F. Mahdi, N.H. Naser, S.M. Ali, Design, synthesis and pharmacological evaluation of sulfanilamide-ciprofloxacin conjugates utilizing hybridization approach as new antibacterial agent, J. Nat. Sci. Res. 5 (2015) 106–117.
[48] A. Tacic, V. Nikolic, L. Nikolic, I. Savi, Antimicrobial sulfonamide drugs, Adv. Tech. 6 (2017) 58–71.

[49] H.S. Athi, B.K. Al-Salami, I.J. Al-Assadi, New azo-azomethine derivative of sulfanilamide: Synthesis, characterization, spectroscopic, antimicrobial and antioxidant activity study, J. Phys.: Conf. Series 1294 (2019), 052033 (13 pp).
[50] M.A. Affan, I.P.P. Foo, B.A. Fosihuddin, E.U.H. Sim, M.A. Hapipah, Synthesis, structural, characterization and toxicity studies of novel organotin (IV) complexes derived from benzoylacetone isonicotinylhydrazone (H_2BAS): X-ray crystal structure of (Me_2Sn(BAS)), The Malay. J. Analy. Sci. 13 (2009) 73–85.
[51] K.T. Mohmudov, R.A. Rahimov, M.B. Babanly, M.N. Kopylovic, A.J.L. Pombeiro, Tautomery and acid-base properties of some azoderivatives of benzoylacetone, J. Mol. Liq. 162 (2011) 84–88.
[52] M. Hatakeyama, Y. Nishiyama, H. Nagatani, H. Okamura, H. Imura, Synergistic extraction equilibirium of lanthanide ions with benzoylacetone and a neutral ligand in an ionic liquid, Solv. Res. Dev. 25 (2018) 79–89.
[53] S. Bhutlacharya, S. Banerjee, S. Chattopadyay, M. Banerjee, Spectrophotometric study of complexation of benzoyl acetone with [60]- and [70] Fullerenses and some other electron acceptors, Chem. Phys. Lett. 393 (2004) 504–510.
[54] A.H.M. Hussein, P.A. Abu-Shanab, S.A.S. Mousa, Benzoylacetone as a building block in neterocyclic synthesis: synthesis of polyfunctionally substituted pyridinethione and its derivavtives, Op. Acc. Lib. J. 2 (2015), e1274 (9pp).
[55] J. Mollin, J. Navratilpva, J. Vicar, Ionization and isomerization of acetylacetone in mixed solvents, Chem. Papers 4 (1987) 471–478.
[56] C.R. Bhattacharjee, M.K. Chandhuri, New developments un chemistry of metal acetylacetone complexes, Proc. Ind. Natu. Sci. Acad. 55 (1989) 194–211.
[57] B.K. Rout, V. Chakravortty, Molecular interaction study on binary mixtures of acetylacetone from excess properties of ultrasonic velocity, viscosity and density at various temperatures, Ind. J. Chem. 33A (1994) 303–307.
[58] M. Bag, P. Chattopadhyay, S. Basu, Estimation of Fe(III) using ^{59}Fe and acetylacetone by substoichiometric isotopes-dilution analysis, Ind. J. Chem. Techn. 19 (2012) 357–460.
[59] S. Kurjica, I. Lozic, M. Pantaler, Thermal decomposition of calcium (II) bis (acetylacetone) n-hydrate, Polimeri 35 (2014) 4–9.
[60] P.G. Umape, V.S. Patil, V.S. Padalkar, K.R. Phatangare, V.D. Gupta, A.B. Thate, N. Sekar, Synthesis and characterization of novel yellow azo dyes from 2-morpholin-4-yl-1,3-thiazol-4(5H)-one and study of their azo–hydrazone tautomerism, Dyes Pigments 99 (2013) 291–298.
[61] J. Geng, Y. Dai, H.-F. Qian, N. Wang, W. Huang, 2-Amino-4-chloro-5-formylthiophene-3-carbonitrile derived azo dyes, Dyes Pigments 117 (2015) 133–140.
[62] K. Nejati, Z. Rezvani, B. Massoumi, Syntheses and investigation of thermal properties of copper complexes with azo-containing Schiff-base dyes, Dyes Pigments 75 (2007) 653–657.
[63] M.A. Gouda, H.F. Eldien, M.M. Girges, M.A. Berghot, Synthesis and antitumor evaluation of thiophene based azo dyes incorporating pyrazolone moiety, J. Saudi Chem. Soc. 20 (2016) 151–157.
[64] D.A. Kennedy, N. Vembu, F.R. Fronczek, M. Devocelle, Synthesis of mutual azo prodrugs of anti-inflammatory agents and peptides facilitated by α-aminoisobutyric acid, The J. Org. Chem. 76 (2011) 9641–9647.
[65] P.F. Lamie, J.N. Philoppes, Design and synthesis of three series of novel antitumor–azo derivatives, Med. Chem. Res. 26 (2017) 1228–1240.
[66] K. Anitha, R. Venugopala, V. Rao, Synthesis and antimicrobial evaluation of metal (II) complexes of a novel bisazo Dye 2, 2 [benzene-13-diyl di (E) diazene 2, 1-diyl] bis (4-chloroaniline), J. Chem. Pharm. Res. 3 (2011) 511–519.
[67] N. Al-Obaidi, O.D. Abdul Sattar, F.F. Hadi, A.S. Ali, B.Th. Zaki, Synthesis and characterization of some azo dyes derived from 4- aminoacetophenone, 1, 4 phenylene diamine and studying its dyeing performance and antibacterial activity, J. Biochem. Tech. 9 (2018) 33–42.
[68] H.R. Allcock, D. Sarah, M.K. Karen, Poly(organophosphazenes) with chromophores as substituent groups, Macromolecules 11 (1978) 357–359.
[69] Issam Ahmed Mohammed, Asniza Mustapha, Synthesis of new azo compounds based on N-(4- Hydroxypheneyl)maleimide and N-(4-methylpheneyl)maleimide, Molecules 15 (2010) 7498–7508.
[70] A. Abu, G.A. El-Fadl, A.B. Abd Mohamad, M. Rashad El-Moiz, Optical constants of $Zn_{1-x}Li_xO$ films prepared by chemical bath deposition technique, Physica B 366 (2005) 44–54.
[71] M.J. Frisch, G.W. Trucks, H.B. Schlegel, G.E. Scuseria, M.A. Robb, J.R. Cheeseman, G. Scalmani, V. Barone, B. Mennucci, G.A. Petersson, H. Nakatsuji, M. Caricato, X. Li, H.P. Hratchian, A.F. Izmaylov, J. Bloino, G. Zheng, J.L. Sonnenberg, M. Hada, M. Ehara, K. Toyota, R. Fukuda, J. Hasegawa, M. Ishida, T. Nakajima, Y. Honda, O. Kitao, H. Nakai, T. Vreven, J.A. Montgomery Jr., J.E. Peralta, F. Ogliaro, M. Bearpark, J.J. Heyd, E. Brothers, K.N. Kudin, V.N. Staroverov, R. Kobayashi, J. Normand, K. Raghavachari, A. Rendell, J.C. Burant, S.S. Iyengar, J. Tomasi, M. Cossi, N. Rega, J.M. Millam, M. Klene, J.E. Knox, J.B. Cross, V. Bakken, C. Adamo, J. Jaramillo, R. Gomperts, R.E. Stratmann, O. Yazyev, A.J. Austin, R. Cammi, C. Pomelli, J.W. Ochterski, R.L. Martin, K. Morokuma, V.G. Zakrzewski, G.A. Voth, P. Salvador, J.J. Dannenberg, S. Dapprich, A.D. Daniels, O. Farkas, J.B. Foresman, J.V. Ortiz, J. Cioslowski, D.J. Fox, Gaussian 09, Revision A.1, Gaussian, Inc., Wallingford, 2009.
[72] M. Miyagawa, N. Akai, M. Nakata, UV-induced photoreaction pathways of salicylic acid: Identification of the fourth stable conformer and ketoketene–water complex, Chem. Phys. Lett. 602 (2014) 52–57.
[73] A.C. Backes, J. Schatz, H. Sieh, GIAO-DFT calculated and experimentally derived complexation-induced chemical shifts of calix[4]arene–solvent inclusion complexes, J. Chem. Soc., Perkin Trans. 2 (2002) 484–488.
[74] J.S. Hadi, Z.A. Abdulnabi, A.M. Dhumad, Synthesis, spectral characterization, thermal analysis and DFT computational studies of 2-(1*H*-indole-3-yl)-5-methyl-1*H*-benzimidazole and their Cu(II), Zn(II) and Cd(II) complexes, Eur. J. Chem. 8 (3) (2017) 252–257.
[75] M. Olejniczak, M. Pecul, B. Champagne, E. Botek, Theoretical investigation on the linear and nonlinear susceptibilities of urea crystal, J. Chem. Phys. 128 (2008), 244713 (3 pp).
[76] R. Karimzadeh, Spatial self-phase modulation of a laser beam propagation through liquids with self-induced natural convection flow, J. Opt. 14 (2012), 095701(9 pp).
[77] K. Ogusu, Y. Kohtani, H. Shao, Laser-induced diffraction rings from an absorbing solution, Opt. Rev. 3 (1996) 232–234.
[78] F.L.S. Cuppo, A.M.F. Neto, S.L. Gomez, P. Palffy-Muhoray, Thermal-lens model compared with the Sheik-Bahae formalism in interpreting Z-scan experiments on lyotropic liquid crystals, J. Opt. Soc. Am. B 19 (2002) 1342–1348.
[79] K. Sendhil, C. Vijayan, M.P. Kothiyal, Low-threshold optical power limiting of cw laser illumination based on nonlinear refraction in zinc tetraphenyl porphyrin, Opt. Las. Tech. 38 (2006) 512–515.
[80] D. Haleshappa, A. Jayarama, C.K. Quah, H.C. Kwong, A novel bromo-substituted thiophene based centrosymmetric crystals: thermal, mechanical, and third order NLO properties for the optical limiting applications, Phys. B 585 (2020), 412083(10 pp).
[81] Shivaraj R. Maidur, Parutagouda Shankaragouda Patil, Linear optical and third-order nonlinear optical properties of anthracene chalcone derivatives doped PMMA thin films, Optik 190 (2019) 54–67.
[82] M.F. Zaini, W.M. Khairul, S. Arshad, M. Abdullah, D.A. Zainuri, R. Rahamathullah, M.I. Rosli, M.S. Abd Aziz, I. Abdul Razak, The structure-property studies and mechanism of optical limiting action of methyl 4-((4-aminophenyl)ethynyl)benzoate crystal under continuous wave laser excitation, Opt. Mat. 107 (2020), 110087(18 pp).
[83] Ahmed S. Al-Asadi, Qusay M.A. Hassan, Amjad F. Abdulkader, H. Bakr, C.A. Emshary, Enhancement of the linear, nonlinear and optical limiting properties of epoxy resin decorated by zinc oxide nanoparticles, Phys. Scr. 95 (2020), 085503 (12pp).
[84] S. Arun Kumar, J. Senthilselvan, G. Vinitha, Third order nonlinearity and optical limiting behaviors of Yb:YAG nanoparticles by Z-scan technique, Opt. Las. Tech. 109 (2019) 561–568.
[85] Kh.A. Al-Timimy, Qusay M.A. Hassan, H.A. Sultan, C.A. Emshary, Solvents effect on the optical nonlinear properties of the sudan iv, Optik 224 (2020), 165398 (15pp).
[86] M. Thangaraj, G. Vinitha, T.C. SabariGirisun, P. Anandan, G. Ravi, Third order nonlinear optical properties and optical limiting behavior of alkali metal complexes of p-nitrophenol, Opt. Las. Tech. 73 (2015) 130–134.
[87] N. Elavarasu, P. Sathya, S. Pugazhendhi, N. Vijayan, K.K. Maurya, R. Gopalakrishnan, Evaluation of suitability of AMT single crystal for optical limiting applications by performing structural, dielectric, mechanical, optical and third order nonlinearity characterization studies, Opt. Las. Tech. 84 (2016) 107–117.